Received: 14 April 2020 | Revised: 27 June 2020 | Accepted: 30 June 2020

DOI: 10.1111/cas.14558

ORIGINAL ARTICLE

Cancer Science WILEY

# Oncogenic mutation in RAS-RAF axis leads to increased expression of *GREB1*, resulting in tumor proliferation in colorectal cancer

Masatoshi Kochi[1] | Takao Hinoi[1,2,3] | Hiroaki Niitsu[4] | Masashi Miguchi[5] | Yasufumi Saito[6] | Haruki Sada[1,2] | Kazuhiro Sentani[7] | Naoya Sakamoto[7] | Naohide Oue[7] | Hirotaka Tashiro[2] | Yusuke Sotomaru[8] | Wataru Yasui[7] | Hideki Ohdan[1]

[1]Department of Gastroenterological and Transplant Surgery, Applied Life Sciences, Institute of Biomedical and Health Sciences, Hiroshima University, Hiroshima, Japan

[2]Department of Surgery, National Hospital Organization Kure Medical Center and Chugoku Cancer Center, Hiroshima, Japan

[3]Department of Clinical and Molecular Genetics, Hiroshima University Hospital, Hiroshima, Japan

[4]Department of Medicine, Vanderbilt University Medical Center, Nashville, TN, USA

[5]Department of Gastroenterological, Breast and Transplant Surgery, Hiroshima Prefectural Hospital, Hiroshima, Japan

[6]Department of Surgery, Chugoku Rosai Hospital, Hiroshima, Japan

[7]Department of Molecular Pathology, Hiroshima University Institute of Biomedical and Health Sciences, Hiroshima, Japan

[8]Natural Science Center for Basic Research and Development, Hiroshima University, Hiroshima, Japan

**Correspondence**
Takao Hinoi, Department of Clinical and Molecular Genetics, Hiroshima University Hospital, Hiroshima, Japan.
Email: thinoi@hiroshima-u.ac.jp

**Funding information**
Japan Society for the Promotion of Science, Grant/Award Number: JP18K08694, JP22390257 and JP25293284

## Abstract

*BRAF*$^{V600E}$ mutation accounts for up to 90% of all *BRAF* mutations in human colorectal cancer (CRC), and constitutively activates the MEK-MAPK pathway. It is recognized that neutralizing mAbs for epidermal growth factor receptor alone are not effective for CRC with *BRAF*$^{V600E}$ mutation. Therefore, there is increasing interest in identification of the possible therapeutic targets in downstream of *BRAF* mutation in CRCs. To address this, we studied genome engineered mouse models for colonic neoplasia that has *Braf*$^{V600E}$ mutation on the basis of *Apc* inactivation, induced in 2 distinct *Cre* mouse models, *CDX2P-G22Cre* and *CDX2P-CreER*$^{T2}$ mice. We carried out oligonucleotide microarray analysis for colonic neoplasia generated in these mouse models, and compared gene expression profiles among *Kras/Braf* WT, *Kras*-mutated, and *Braf*-mutated mouse colon tumors to seek new molecular targets corresponding to the KRAS-BRAF-MAPK axis. We found that the expression of the growth regulation by estrogen in breast cancer protein 1 (*Greb1*) was the most upregulated gene in *Braf*-mutated mouse tumors compared to *Kras/Braf* WT counterparts. The silencing

**Abbreviations:** AF, activation factor; Apc, adenomatous polyposis coli; CIMP, CpG island methylator phenotype; CRC, colorectal cancer; EGFR, epidermal growth factor receptor; ER, estrogen receptor; GEMM, genome engineered mouse model; GREB1, growth regulation by estrogen in breast cancer protein 1; HGSOC, high-grade serous ovarian cancer; IHC, immunohistochemical; MSI, microsatellite instability; MSS, microsatellite stable; qRT-PCR, quantitative RT-PCR; RIN, RNA integrity number; TAM, tamoxifen.

This is an open access article under the terms of the Creative Commons Attribution-NonCommercial License, which permits use, distribution and reproduction in any medium, provided the original work is properly cited and is not used for commercial purposes.
© 2020 The Authors. Cancer Science published by John Wiley & Sons Australia, Ltd on behalf of Japanese Cancer Association

of *GREB1* significantly reduced the proliferation and tumorigenesis of CRC cell lines, whereas the overexpression of *GREB1* promoted cell proliferation. Although *GREB1* was first identified as a hormone-responsive gene mediating estrogen-stimulated cell proliferation in endometriosis, breast, and ovarian cancers, these results suggest that RAS-RAF-MAPK signaling upregulates *GREB1* expression in CRC, resulting in cellular proliferation. Thus, *GREB1* is a possible therapeutic target for CRCs with *Braf*$^{V600E}$ mutation.

**KEYWORDS**
BRAF mutation, colorectal cancer, ER, GREB1, mouse model

## 1 | INTRODUCTION

Human CRCs evolve by a series of genetic aberrations accumulated over time.[1,2] Although the genetic abnormality varies among individual tumors, dysregulation of Wnt/β-catenin and EGFR signaling pathway plays a major role in CRC,[1] thus, are thought to be therapeutic targets. Cetuximab and panitumumab are EGFR-mAbs, clinically approved for the treatment of advanced CRCs.[3] However, 40%-50% of CRCs have *KRAS/NRAS* mutation, resulting in resistance to these EGFR-mAbs due to constitutive activation of a RAS-RAF-MAPK signaling pathway.[3-5]

*BRAF* mutation is a driver gene mutation that constitutively activates the MEK-MAPK signal pathway at the downstream of RAS. Colorectal cancers with *BRAF* mutation are thus resistant to EGFR-mAbs.[6] As *BRAF*$^{V600E}$ mutation accounts for approximately 90% of all *BRAF* mutations in CRC,[7] vemurafenib, a specific serine/threonine kinase inhibitor for V600E-mutated BRAF, has been clinically tested.[8-11] However, the survival benefit is still unsatisfactory.[12]

CpG island methylator phenotype-high frequently presents with *BRAF* mutation and causes hypermethylation of *MLH1* promoter, resulting in MSI-high.[13] In contrast, MSS and CIMP-low CRCs are less frequent, resulting in worse prognosis than the aforementioned CIMP-high/MSI-high/*BRAF*-mutated CRCs.[14] Those types of CRCs are distinct, and therefore, *BRAF* mutation in CRCs should be studied in the context of CIMP or microsatellite status.

We developed 2 different GEMMs for colon cancer, the *CDX2P-G22-Cre*;*Apc*$^{flox/flox}$ and *CDX2P-Cre-ER*$^{T2}$;*Apc*$^{flox/flox}$ models. In these 2 GEMMs, colonic tumors occur with inactivation of both LoxP-flanked *Apc* alleles induced by *CDX2P*-driven Cre recombinase. *CDX2P-G22-Cre*;*Apc*$^{flox/flox}$ mice express Cre when frame-shift mutation occurs in G22 tracts followed by Cre locus, which appear to recapitulate MSI-high tumors.[15] In contrast, *CDX2P-Cre-ER*$^{T2}$;*Apc*$^{flox/flox}$ is less similar to an MSI-high model.[16] Therefore, these 2 mouse models are useful to test the effect of *Braf* mutation in the context of MSI-high and MSS.

As previously described, we have already studied GEMMs that generate proximal colon tumors with or without *Kras*$^{G12D}$ mutation induced in the *CDX2P-G22-Cre* model, and compared the gene expression profiles to seek the possible molecules that are regulated downstream of *Kras* mutation.[17,18] Mimicking this strategy, we first established GEMMs that generate colonic tumors with or without *Braf*$^{V600E}$ mutation. Subsequently, we carried out gene expression profiling, and integrated gene expression profiles of *Kras/Braf* WT, *Kras*-mutated, and *Braf*-mutated mouse colon tumors to seek new molecular targets corresponding to the KRAS-BRAF-MAPK axis.

## 2 | MATERIALS AND METHODS

### 2.1 | Ethics statement

This study was undertaken in strict accordance with the Guide for the Care and Use of Laboratory Animals and the committee of the University of Hiroshima.

This study was approved by the Ethical Committee for Epidemiology of Hiroshima University (Permit Number: Epidemiology-744).

### 2.2 | Experimental animals

All mice were housed under specific pathogen-free conditions, as described previously.[17] We utilized 2 different kinds of Cre mice, *CDX2P-G22Cre* and *CDX2P-CreER*$^{T2}$, as described previously and above.[15,16] These Cre mice were crossed with *Apc*$^{flox/flox}$ mice and *Braf*$^{LSL-V600E/+}$ mice (C57BL/6J),[19] to obtain *CDX2P-G22Cre*;*Apc*$^{flox/flox}$;*Braf*$^{LSL-V600E/+}$, *CDX2P-G22Cre*;*Apc*$^{flox/flox}$, *CDX2P-CreER*$^{T2}$;*Apc*$^{flox/flox}$;*Braf*$^{LSL-V600E/+}$, and *CDX2P-CreER*$^{T2}$;*Apc*$^{flox/flox}$ mice. Experiments were carried out using these mice and previously described *CDX2P-G22Cre*;*Apc*$^{flox/flox}$;*Kras*$^{LSL-G12D/+}$ mice.[18]

Tamoxifen (Sigma-Aldrich) was dissolved in 10 mg/mL corn oil, and single doses of 15 mg/kg TAM were i.p. injected into mice with the *CDX2P-CreER*$^{T2}$ transgene at the age of 6 weeks. Animals were killed and analyzed at various time points after the single injection.

### 2.3 | Tissue harvesting and fixation

Small intestine and colon were harvested and then washed with PBS containing 0.01% Triton-X100 at 4°C for 30-60 minutes on a shaker.

For histological analyses, specimens were fixed in 4% paraformaldehyde and then embedded in paraffin. For RNA extraction from tissue with laser capture microdissection, specimens without any fixation were embedded and frozen in optimal cutting temperature compound (Sakura Finetek Japan), and stored at −80°C.

## 2.4 | Laser capture microdissection and gene expression profiling

First, 12 μm frozen sections were prepared, dehydrated, and stained with hematoxylin. Subsequently, cancer tissues were dissected with the LMD6500 laser capture microdissection device (Leica Microsystems), from which RNA was immediately extracted with an RNeasy Micro Kit (Qiagen).

The quality of extracted total RNA was evaluated by RIN, which is calculated with Bioanalyzer (Agilent 2100). RNA sample scoring RIN > 6.0 were used for the following microarray analysis.

Gene expression profiling was compared among *CDX2P-G22Cre*;*Apc*$^{flox/flox}$;*Braf* $^{LSL\text{-}V600E/+}$ (n = 3), *CDX2P-G22Cre*;*Apc*$^{flox/flox}$;*Kras*$^{LSL\text{-}G12D/+}$ (n = 3), and *CDX2P-G22Cre*;*Apc*$^{flox/flox}$ (n = 3) mouse tumors with a Mouse Gene 1.0 ST Array (Affymetrix). The arrays were scanned using a GeneArray scanner (Affymetrix), and gene expression data were analyzed using GeneSpring GX software version 11 (Agilent Technology). The robust multichip analysis algorithm was used for normalization to remove artifactual differences between arrays, and cut-off values were set at less than 20% to eliminate poorly reproducible entities between chips.

## 2.5 | Quantitative RT-PCR

cDNA was generated using a QuantiTect Reverse Transcription Kit (Qiagen) and was analyzed with a Rotor-Gene Q 2PLEX HRM Real-Time PCR system (Qiagen). The PCR primers used for gene analysis are shown in Table S1.

## 2.6 | Immunohistochemistry and immunofluorescence

For human tissues, formalin-fixed paraffin-embedded samples were sectioned to 5-μm-thick sections and stained for GREB1 using a Catalyzed Signal Amplification System (Dako Japan), which is based on a streptavidin-biotin-HRP complex formation. After deparaffinization and rehydration, the sections were treated with target retrieval solution (Dako Japan) (pH 9.0) at 96°C for 40 minutes. A rabbit anti-human GREB1 polyclonal Ab (sc-138794; Santa Cruz Biotechnologies) was used at a dilution of 1:100, followed by incubation with peroxidase-labeled anti-rabbit IgG for 60 minutes. Immunocytofluorescence staining for FLAG was done with a primary Ab anti-Flag M2 (clone M2, 1:50; Sigma-Aldrich) and the secondary Ab Alexa 546 Donkey Anti-mouse IgG (diluted 1:500; Thermo Fisher Scientific). Cells were then stained with DAPI (diluted 1:10 000; Thermo Fisher Scientific), and cover-slips were mounted onto microscope slides in the presence of a Mowiol mounting medium. Fluorescence images were captured with an Olympus IX81 microscope.

## 2.7 | Western blot analysis

Western blot analysis was carried out as described previously.[20,21] Whole cell lysate was prepared with 1.0% SDS containing protease inhibitors (complete mini protease inhibitor cocktail tablet; Sigma-Aldrich). Anti-GREB1 polyclonal Ab (ab72999, Abcam) and anti-β-actin mAb (clone AC-15; Sigma–Aldrich) were used at 1:1000 dilutions for GREB1.

## 2.8 | Surgical specimens

Formalin-fixed paraffin-embedded specimens of human CRC were obtained from 77 patients who had undergone colectomy at Hiroshima University Hospital between 2006 and 2011 and were used for GREB1 IHC analyses. Written informed consent for participation in the study was obtained from all participants.

## 2.9 | Plasmid construction

A 2301-bp fragment of the *BRAF* allele was amplified by PCR using cDNA from colon cancer cells with the *BRAF* mutation (V600E) and then inserted into the retroviral vector pDON-5 neo (Takara Bio) to generate the pDON-5/*BRAF*$^{V600E}$ vector. The pDON-5/*KRAS*$^{G12D}$ vector was generated in the same manner.

A 5850-bp fragment of the *GREB1* allele containing a Flag tag at the 3′-end was amplified by PCR using cDNA from MCF-7 cells and then inserted into the retroviral vector pDON-5 neo to generate the pDON-5/*GREB1* vector. Hairpin-loop oligonucleotides targeting *GREB1* and a nonsilencing sequence were synthesized and inserted into pSUPER.retro. neo + gfp (OligoEngine) to generate pSUPER/*GREB1* shRNA and pSUPER/non-silencing shRNA (Table S2).

## 2.10 | Cell lines and retroviral infections

All cell lines, SW48 (PRID: CVCL_1724), Caco2 (PRID: CVCL_0025), RKO (PRID: CVCL_0504), Hct116 (PRID: CVCL_0291), MCF-7 (PRID: CVCL_0031), and Colo320 (PRID: CVCL_1989) were obtained from ATCC. AmphoPack-293 (Takara Bio, PRID: CVCL_WI47) cells were transfected with retroviral constructs; and supernatants containing nonreplicating amphotropic virus were harvested.

For induction of *BRAF*$^{V600E}$ and *KRAS*$^{G12D}$ mutations, SW48 and Caco2 cells, in which *KRAS* and *BRAF* are known to be

WT, were infected with virus containing pDON-5/*BRAF*$^{V600E}$, *KRAS*$^{G12D}$ and empty vectors. For GREB1 overexpression, RKO cells were infected with virus containing pDON-5/*GREB1* and pDON-5 vectors. For *GREB1* silencing, Hct116 cells, in which endogenous *GREB1*-mRNA was confirmed to be high, were infected with virus containing pSUPER/*GREB1* shRNA and pSUPER/nonsilencing shRNA. Cells were selected with neomycin (500 μg/mL for RKO and Hct116 cells) for 2-5 weeks, as previously described.[21]

### 2.11 | Cell proliferation assays

Cellular proliferation was measured using a brightfield image label-free high-content time-lapse assay with the IncuCyte Zoom system (Essen BioScience) according to the manufacturer's instructions. Cell viability was also measured with MTS-based CellTiter 96 AQueous One Solution Reagent (Promega), as described previously.[17,21]

### 2.12 | Soft agar colony formation assays

The ability of knockdown *GREB1* or nonsilencing cells (Hct116) to form macroscopically visible colonies in soft agar was determined essentially as described previously.[22]

### 2.13 | In vivo tumorigenesis assays

Female BALB/cA Jcl-nu/nu mice (CLEA Japan) were used at 5 weeks of age. A total of $5.0 \times 10^6$ Hct116 cells (*GREB1* knockdown or nonsilencing) and RKO cells (*GREB1* overexpression or empty) were s.c. injected into the right flanks of 8 nude mice. The tumors were removed and weighed on day 14.

### 2.14 | *BRAF*$^{V600E}$ mutant and *BRAF* WT patient cohort

The effect of *BRAF*$^{V600E}$ mutation on *GREB1* expression in human CRC was analyzed using The Cancer Genome Atlas dataset (accession number: phs000178) for colorectal adenocarcinoma (COADREAD).

### 2.15 | Statistical analysis

The statistical significance of differences was determined by Mann-Whitney *U* test, $\chi^2$ test, unpaired *t* test, or Fisher's exact test. Differences with a *P* value of less than .05 were considered statistically significant. All statistical analyses were undertaken using JMP 12 software (SAS Institute).

## 3 | RESULTS

### 3.1 | *CDX2P-G22Cre;Apc*$^{flox/flox}$*;Braf*$^{LSL\text{-}V600E/+}$ and *CDX2P-CreER*$^{T2}$*;Apc*$^{flox/flox}$*; Braf* $^{LSL\text{-}V600E/+}$ mice developed polypoid lesions, including well to moderately differentiated adenocarcinoma, in the proximal colon

In the *G22Cre* mouse model, genetic analysis showed evidence of recombination of the *Apc*$^{flox}$ and *Braf*$^{LSL\text{-}V600E}$ alleles in the tumor tissue, but not in the small intestine or normal tissue of colon (Figure 1A). Median survival time of *CDX2P-G22Cre;Apc*$^{flox/flox}$*;Braf*$^{LSL\text{-}V600E/+}$ and *CDX2P-G22Cre;Apc*$^{flox/flox}$ mice was 8.5 weeks and 19.1 weeks, respectively (Figure 1B). Histologically, *CDX2P-G22Cre;Apc*$^{flox/flox}$*;Braf*$^{LSL\text{-}V600E/+}$ and *CDX2P-G22Cre;Apc*$^{flox/flox}$ mice generated high-low and low-grade adenoma, respectively, but no invasions to the submucosa, lymph node metastases, or distant metastases were observed (Figure 1C-H). Body weights of both *CDX2P-CreER*$^{T2}$*;Apc*$^{flox/flox}$*;Braf* $^{LSL\text{-}V600E/+}$ and *CDX2P-CreER*$^{T2}$*;Apc*$^{flox/flox}$ mice were measured every week after TAM injections. *CDX2P-CreER*$^{T2}$*;Apc*$^{flox/flox}$*;Braf* $^{LSL\text{-}V600E/+}$ mice showed significantly lower body weights from 9 week after the injection of TAM (Figure 1I). Similarly, in comparison to *CDX2-G22Cre* mice, the median survival time of *CDX2P-CreER*$^{T2}$*;Apc*$^{flox/flox}$*;Braf* $^{LSL\text{-}V600E/+}$ and *CDX2P-CreER*$^{T2}$*;Apc*$^{flox/flox}$ mice was 13.0 weeks and 26.5 weeks, respectively (Figure 1J). Results consistent with the *CDX2-G22Cre* mouse model were also observed for *CDX2P-CreER*$^{T2}$ mouse model (Figure 1K-P). We carried out IHC staining of Ki67, Cdx2, β-catenin, and p53 (Figure S1).

### 3.2 | Identification of candidate genes whose expression was altered in response to *Braf* mutation by microarray analysis

In gene expression profiles from the oligonucleotide microarray, between *CDX2P-G22Cre;Apc*$^{flox/flox}$*;Braf*$^{LSL\text{-}V600E/+}$ (*Braf* MT) and *CDX2P-G22Cre;Apc*$^{flox/flox}$ (*Braf/Kras* WT) mice, differentially expressed genes of the tumor ($P < .05$) were identified as those having a fold change of at least 2.0 (upregulated gene) or −4.0 (downregulated gene). Five genes were significantly upregulated, and 8 genes were significantly downregulated in the tumors of *CDX2P-G22Cre;Apc*$^{flox/flox}$*;Braf*$^{LSL\text{-}V600E/+}$ mice. Similar results were obtained for all candidate genes in the comparison between *CDX2P-G22Cre;Apc*$^{flox/flox}$*;Kras*$^{LSL\text{-}G12D/+}$ mice and *CDX2P-G22Cre;Apc*$^{flox/flox}$ mice. It was suggested that these genes might be regulated by the RAS-RAF axis (Table 1).

Quantitative RT-PCR was subsequently carried out to validate expression changes in these 13 candidate genes (Figure S2). The genes that were indicated to be increased or decreased in qRT-PCR both in *G22Cre* and *CreER*$^{T2}$ mouse model were *Greb1*, *Abcb1a*, *Cyp2s1*, and *Bex1*. Of these candidates, we decided to further investigate *Greb1*, because the fold change of *Greb1* was the largest among the 4 candidates.

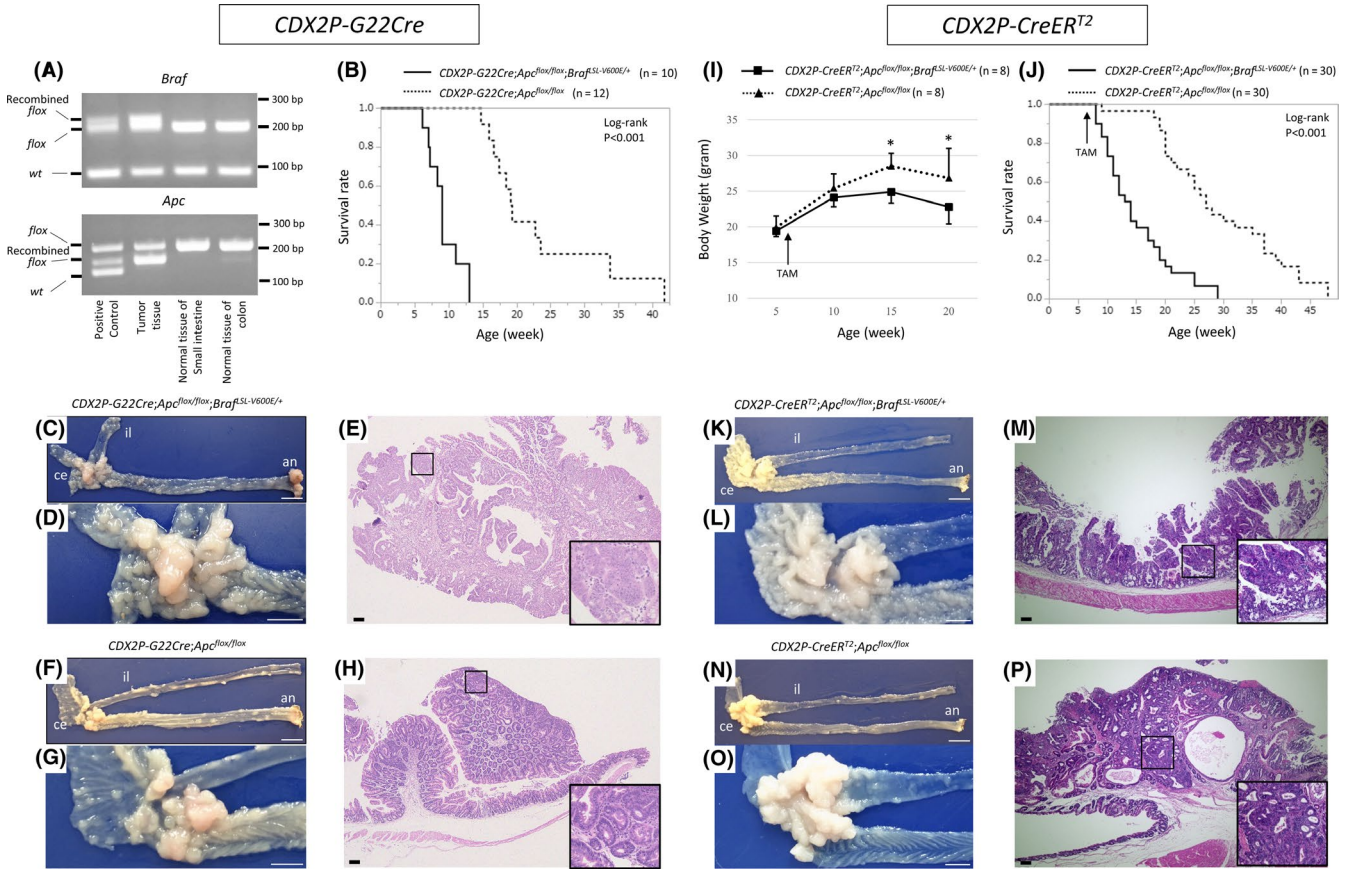


**FIGURE 1** Tumorigenesis in *CDX2P-G22Cre;Apc*$^{flox/flox}$;*Braf*$^{LSL\text{-}V600E/+}$ and *CDX2P-CreER*$^{T2}$;*Apc*$^{flox/flox}$;*Braf*$^{LSL\text{-}V600E/+}$ mice, and histological analysis of tumors. A, Genotyping of *Braf* and *Apc* in tumor, normal jejunum, and normal colon tissues. B, J, Survival times were shortened in *Braf*$^{V600E}$ mutation induced by 2 distinct Cre mouse models relative to *Braf* WT mouse models. Solid line, *Braf* mutation mice; dotted line, *Braf* WT mice. C-H, K-P, Extensive polyposis in the cecum and proximal colon was observed in *CDX2P-G22Cre;Apc*$^{flox/flox}$;*Braf*$^{V600E/+}$ mice (C, D), *CDX2P-G22Cre;Apc*$^{flox/flox}$ mice (F, G), *CDX2P-CreER*$^{T2}$;*Apc*$^{flox/flox}$;*Braf*$^{V600E/+}$ mice (K, L), and *CDX2P-CreER*$^{T2}$;*Apc*$^{flox/flox}$ mice (N, O). High-low-grade adenomas were generated in *CDX2P-G22Cre;Apc*$^{flox/flox}$;*Braf*$^{V600E/+}$ mice (E) and *CreERT*$^{2}$;*Apc*$^{flox/flox}$;*Braf*$^{V600E/+}$ mice (M). Low-grade adenomas were generated in *CDX2P-G22Cre;Apc*$^{flox/flox}$ mice (H) and *CDX2P-CreERT*$^{2}$;*Apc*$^{flox/flox}$ (P) mice. an, anus; ce, cecum; il, ileum. Scale bars: 10 mm (C, F, K, N), 5 mm (D, G, L, O), 100 μm (E, H, M, P). I, Body weights of 10- and 15 wk-old male mice were lower in *CDX2P-CreER*$^{T2}$;*Apc*$^{flox/flox}$; *Braf*$^{V600E/+}$ mice than in *CDX2P-CreER*$^{T2}$;*Apc*$^{flox/flox}$ mice. Points, means; bars, SDs

## 3.3 | *BRAF*$^{V600E}$ and *KRAS*$^{G12D}$ mutation led to an increase of mRNA levels of *GREB1* in CRC cell lines

To investigate the impact of mutant *BRAF* and mutant *KRAS* on the expression of *GREB1* in vitro, SW48 and Caco2 in which *BRAF*$^{V600E}$ and *KRAS*$^{G12D}$ were analyzed in terms of *GREB1*-mRNA expression by qRT-PCR, and induction of *BRAF*$^{V600E}$ and *KRAS*$^{G12D}$ resulted in higher expression level of *GREB1* in both cell lines (Figure 2).

## 3.4 | Effects of *GREB1* knockdown on cell growth

We analyzed the effects of GREB1 expression on proliferative ability by *GREB1* knockdown in CRC cell lines. Quantitative RT-PCR confirmed that the shRNA significantly blocked GREB1 expression compared with that in cells transfected with non-silencing RNA (Figure 3A; $P < .05$).

For evaluation of cellular proliferation ability, MTS cell viability assays and time-lapse cell proliferation assays with the IncuCyte Zoom system were carried out, both of which consistently indicated that knockdown of *GREB1* was associated with lower proliferation than that in nonsilencing control groups (Figure 3B,C). To evaluate whether this proliferative ability is in an anchor-independent manner, soft agar colony formation assays were then undertaken, in which *GREB1* knockdown resulted in a significant decrease in anchorage-independent growth ability (Figure 3D,E: *GREB1* knockdown cells, 173.3 ± 39.5 colonies per well; and nonsilencing cells, 337.3 ± 32.3 colonies per well ($P < .05$). Furthermore, we implanted *GREB1* knockdown cells or nonsilencing cells into 8 nude mice for in vivo tumorigenesis assays. Tumor volume was significantly smaller in the *GREB1* knockdown group than in the nonsilencing group (Figure 3F,H; 45.4 ± 61.9 vs 146.4 ± 110.4 mm$^3$, respectively; $P < .05$). Likewise, tumor weights were significantly reduced in mice inoculated with *GREB1* knockdown cells compared with that in mice inoculated with nonsilencing cells (Figure 3G,H; 29.8 ± 36.4 vs 83.0 ± 57.3 mg, respectively; $P < .05$).

**TABLE 1** Gene expression profiling using microarray analysis for *Braf*-mutated (MT), *Kras*-MT, and *Braf/Kras* WT mouse models

| Gene symbol | Function | *Braf* MT vs *Braf/Kras* WT, fold | *Kras* MT vs *Braf/Kras* WT, fold | Validation (*G22Cre*), *P* value | Validation (*CreER*$^{T2}$), *P* value |
|---|---|---|---|---|---|
| Upregulated genes | | | | | |
| *Greb1* | Promote cell proliferation | 4.5 | 3.9 | 0.009 | 0.016 |
| *Eda2r* | Activate protein of NFKB and JNK | 4.0 | 3.5 | 0.009 | 0.075 |
| *Abcb1a* | Intestinal epithelial barrier function | 3.3 | 2.1 | 0.016 | 0.028 |
| *Cyp2s1* | Metabolic enzyme | 3.1 | 1.7 | 0.047 | 0.009 |
| *Nox1* | Enzymes function to generate physiological levels of ROS | 2.6 | 1.4 | 0.117 | 0.117 |
| Downregulated genes | | | | | |
| *Lrg1* | regulator of angiogenesis | −14.3 | −3.5 | 0.009 | 0.347 |
| *Gkn3* | Regulator of cell proliferation | −7.6 | −4.8 | 0.009 | 0.601 |
| *Ltf* | Iron-binding glycoprotein of the transferrin | −7.3 | −4.0 | 0.009 | 0.174 |
| *Muc6* | Secreted glycoprotein | −6.6 | −3.3 | 0.075 | 0.028 |
| *Lcn2* | Protein associated with neutrophil gelatinase | −6.1 | −1.7 | 0.009 | 0.174 |
| *Lgr5* | Receptors for glycoprotein hormones | −5.3 | −1.9 | 0.028 | 0.117 |
| *Bex1* | Regulator of cell cycle | −4.0 | −3.5 | 0.009 | 0.028 |
| *Lum* | Interacts with collagen and limits growth of fibrils | −4.0 | −2.4 | 0.624 | 0.250 |

Fold change *Braf* MT vs *Braf/Kras* WT: Fold indicates a gene expression ratio of the tumors of *CDX2P-G22Cre;Apc*$^{flox/flox}$;*Braf*$^{V600E/+}$ mice to those of *CDX2P-G22Cre;Apc*$^{flox/flox}$ mice.

Fold change *Kras* MT vs *Braf/Kras* WT: Fold indicates a gene expression ratio of the tumors of *CDX2P-G22Cre;Apc*$^{flox/flox}$;*Kras*$^{GnD/+}$ mice to those of *CDX2P-G22Cre;Apc*$^{flox/flox}$ mice.

Validation: Results of quantitative RT-PCR between *Braf* MT and *Braf/Kras* WT mouse tumor in each *Cre* mouse model.

Abbreviations: JNK, c-Jun N-terminal Kinase; NFKB, nuclear factor-κB; ROS, reactive oxygen species.

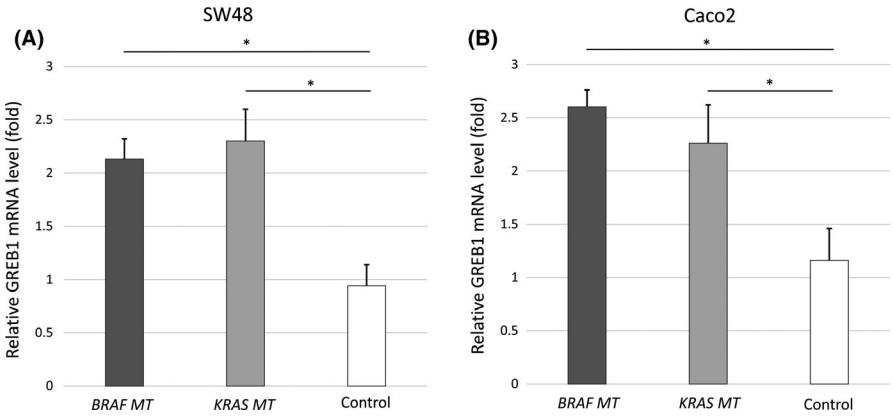


**FIGURE 2** Expression levels of *GREB1* mRNAs in SW48 and Caco2 cells (quantitative RT-PCR). SW48 and Caco2 cells overexpressing BRAF$^{V600E}$ or KRAS$^{G12D}$ showed significantly higher expression of *GREB1* compared with control cells. Representative data from 5 independent experiments are shown. *$P < .05$. Data are expressed as mean ± SD

## 3.5 | Effects of GREB1 overexpression on cell growth

RKO cells were transfected with a vector encoding human full-length *GREB1* (pDON-5/*GREB1*) or an empty vector (pDON-5). The efficiency of GREB1 overexpression is shown in Figure 3I,J.

The proliferation assays carried out using the IncuCyte Zoom system revealed that cell proliferation was significantly increased in the GREB1 overexpression group compared with that in the empty vector group (Figure 3K; $P < .05$). We also undertook a skin

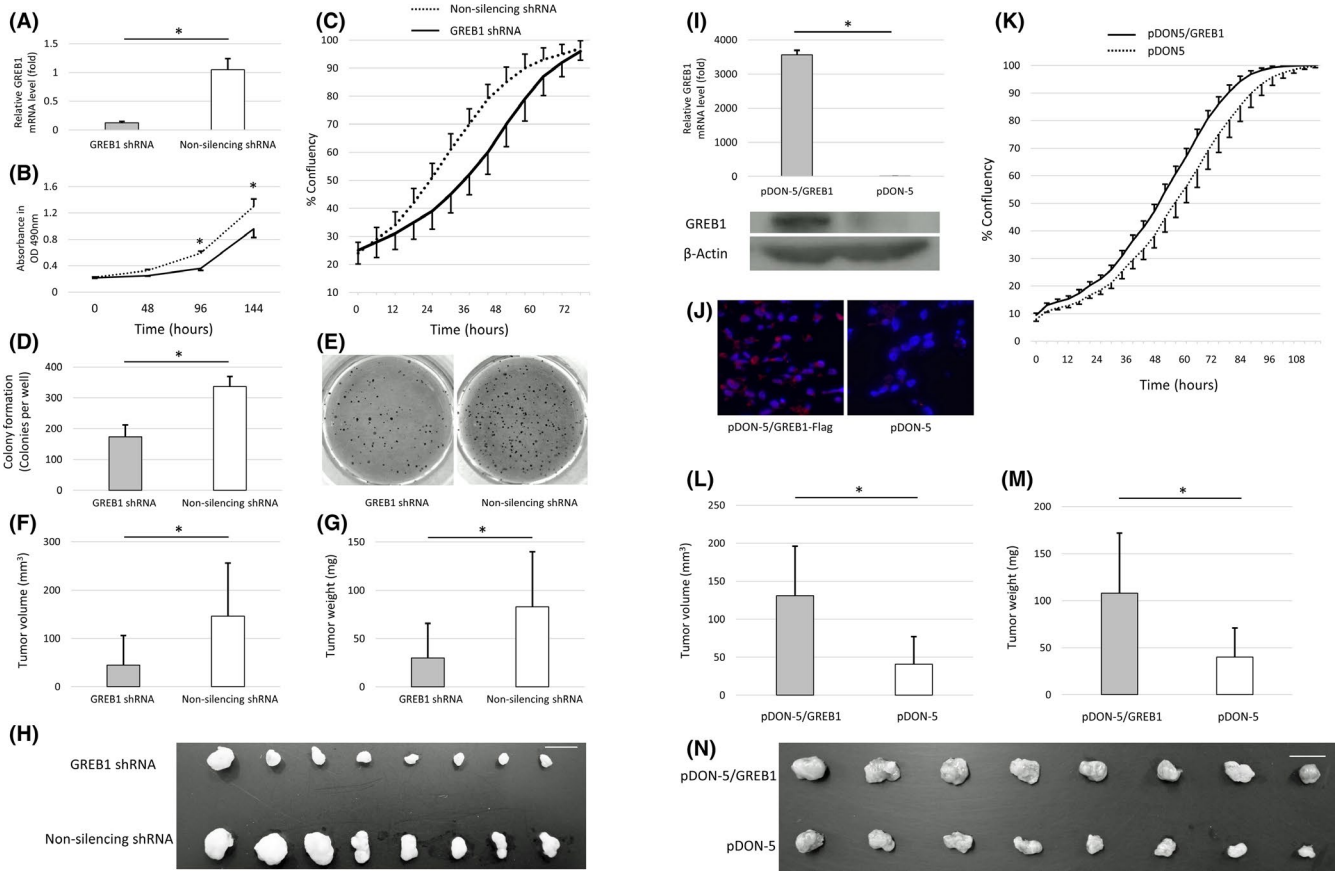


**FIGURE 3** *GREB1* promoted tumor growth in vitro and in vivo. A, Quantitative RT-PCR of the expression of *GREB1* mRNA of Hct116 cells infected with pSUPER/*GREB1* shRNA and pSUPER/nonsilencing shRNA. *$P < .05$. B, MTS assays were used to analyze the effects of *GREB1* stable knockdown on cell proliferation in Hct116 cells for up to 6 d. *$P < .05$. C, Proliferation was compared in Hct116 cells with or without *GREB1* stable knockdown. Solid line, *GREB1* shRNA; dotted line, control. D, E, Colony formation assays in Hct116 cells. Number of colonies (D), and imaging results (E). Colonies were monitored for up to 21 d after cell seeding on the plates. Representative data from 3 independent experiments are shown. *$P < .05$. F-H, Effects of *GREB1* stable knockdown in Hct116 cells on the growth of xenograft tumors in nude mice (n = 8). Tumor volume (F) and weights (G) are shown. Volume was determined by the formula $V = 1/2\ L \times W^2$, where L is the length and W is the width. Scale bar = 10 mm. *$P < .05$. I, Upper panel: quantitative RT-PCR of the expression of *GREB1* mRNA of RKO cells infected with pDON-5/*GREB1* or pDON-5. Lower panel: western blot analysis. *$P < .05$. J, Immunofluorescence staining of tumors from RKO cells transfected with pDON-5/ GREB1-Flag or pDON-5 by anti-FLAG Ab. Nuclei stained by DAPI are shown in blue, and FLAG stained by Alexa 546 are shown in red. Left panel: overexpression of GREB1 was detected in RKO cells transfected with pDON-5/ *GREB1*. Right panel: control. Scale bar = 10 μm. K, Proliferation was compared in RKO cells transfected with pDON-5/ *GREB1* or pDON-5. Solid line, pDON-5/*GREB1*; dotted line pDON-5. L-N, Effects of GREB1 overexpression in RKO cells on the growth of xenograft tumors in nude mice (n = 8). Tumor volume (L) and weights (M) are shown. Volume was determined by the formula $V = 1/2\ L \times W^2$, where L is the length and W is the width. Scale bar = 10 mm. *$P < .05$

xenograft in vivo tumorigenesis assay GREB1-overexpressed and empty vector-induced control cells. Tumor volumes and weight were larger and heavier in the GREB1-overexpressed group than in the control group (Figure 3L-N; size, 131.1 ± 41.5 vs 65.3 ± 36.6 $mm^3$, respectively, $P < .05$; weight, 108.7 ± 40.7 vs 64.8 ± 31.1 mg, respectively, $P < .05$).

### 3.6 | Strong GREB1 expression predicts poor prognosis in CRC patients

We analyzed the expression of GREB1 protein in human colorectal cancer (CRC) specimens (Figure 4A-D). Immunohistochemical analyses for surgical specimens of human CRCs showed that 37 (48.1%) of the 77 CRC cases showed positive results for GREB1 (cut-off, greater than 30%), and the expression of GREB1 protein was higher in tumor tissues than in adjacent normal tissue (Figure 4B-D). The expression of *GREB1* mRNA was significantly increased in $BRAF^{V600E}$ tumor tissues compared with *BRAF* WT tumor tissues (Figure 4E).

In terms of prognosis, we found GREB1-positive CRCs showed lower overall survival rates than GREB1-negative ones (Figure 4F). In this study, a significant difference was detected at cut-off of 30%. The other cut-offs (10%, 50%, and 80%) did not show a significant difference, although a tendency was recognized (data not shown). In multivariate analyses for prognosis, GREB1, as well as lymphatic

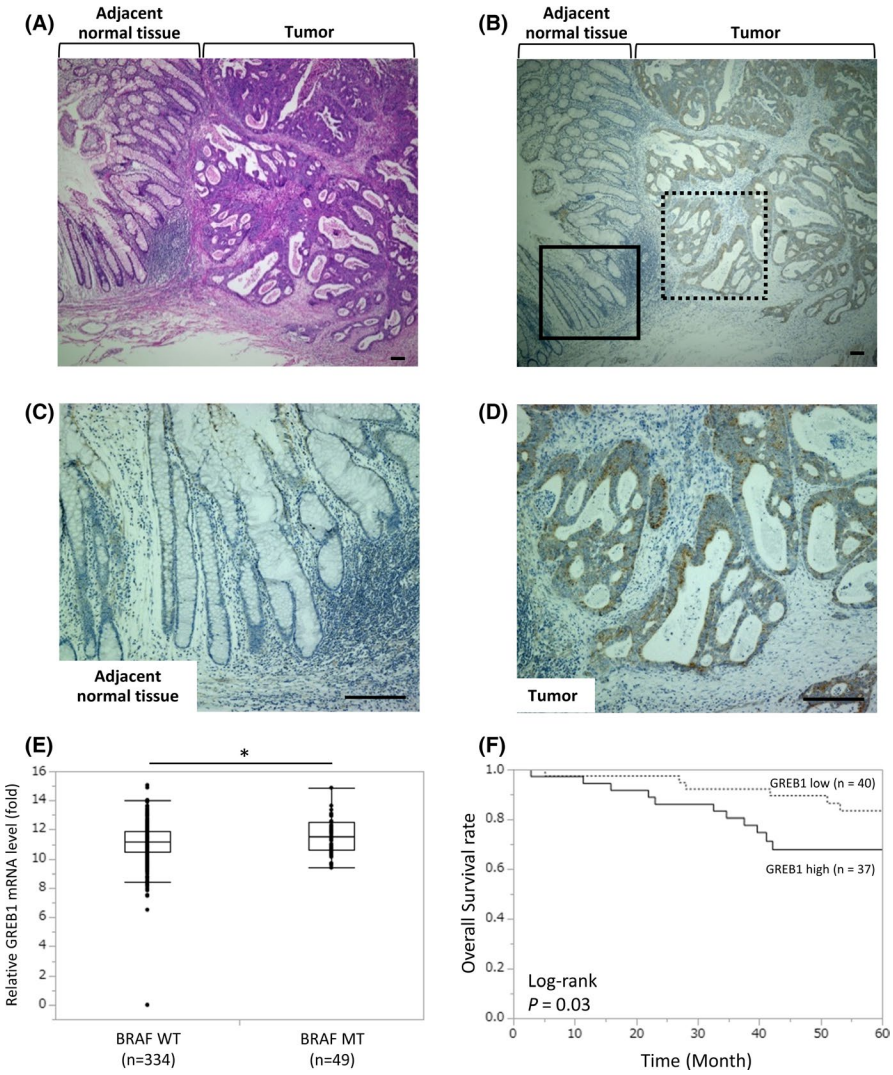


**FIGURE 4** Expression of GREB1 protein and transcript in human colorectal cancer (CRC) specimens. A, Histological findings of surgical specimens from patients with CRC (H&E stain). B-D, Immunohistochemical analyses of GREB1. Expression of GREB1 protein was higher in tumor than in adjacent noncancerous tissue (B). Images of higher magnification of normal tissue (C) and tumor (D) are shown. Representative images of immunohistochemical staining are shown. Scale bar = 100 μm. E, Expression of *GREB1* mRNA was significantly increased in *BRAF*$^{V600}$ tumors compared with *BRAF* WT tumors. Data are shown as box plots. The horizontal lines represent the median scores, the bottom and top of the boxes represent the 25th and 75th percentiles, respectively, and the whiskers represent the range of expression level. *$P < .05$. F, Overall survival rates of the GREB1-high expression group (>30%) and GREB1-low expression group (≤30%)

invasion, was revealed as the independent prognostic factor in CRC (Table 2).

## 4 | DISCUSSION

In this study, we generated a CRC mouse model in which there is biallelic *Apc* inactivation and oncogenic gain-of-function mutations in *Braf* in the colon epithelium; these mutations induce the formation of adenocarcinomas in the proximal colon. We then identified *Greb1* as a novel gene upregulated by either *Kras*$^{G12D}$ or *Braf*$^{V600E}$ mutation induced by 2 distinct Cre mouse models for mouse colonic neoplasia.

*GREB1* was partially discovered from the human brain cDNA library encoding large proteins located in the short arm of chromosome 12 (p25.1), where it spans roughly 108 kb,[23] and a complete sequence of *GREB1* cDNA was identified as a primary target for ER regulation in estradiol-stimulated breast cancer cell line MCF-7. *GREB1* transcript codes for a putative 1949-aa protein with at least 4 transmembrane domains and an N-myristoylation domain.[24] Although *GREB1* was first identified as a hormone-responsive gene, it stands out as an oncogene, which mediates estrogen-stimulated cell proliferation in endometriosis, breast, and ovarian cancers. Therefore, *GREB1* has been considered as a candidate clinical marker for response to endocrine therapy as well as a potential therapeutic target.[25-27] Similarly, *GREB1* might play an important role as an oncogene in prostate cancer growth and could be a prognostic marker as well as predictive marker of androgen responsiveness.[28] These results highlight the important role of *GREB1* as a novel mediator in tumor progression that is a hormone-responsive gene and functions as an oncogene.[26]

In the current study, our data indicated that GREB1 promoted proliferation and tumorigenesis in CRC cell lines in vitro as well as in a mouse xenograft model. Although little is known about the contribution of GREB1 to CRC, it was suggested that high expression of GREB1 protein might be a poor prognostic factor in our CRC cases (Figure 4).

To elucidate the mechanism by which oncogenic *BRAF* upregulates *GREB1* expression, it is important to understand how ER modulates the signaling pathway from the upper molecule to its downstream targets. The molecular structure of ER has 2

**TABLE 2** Results of univariate and multivariate analyses of prognostic factors for overall survival of 5 years in patients with colorectal cancer

| | Univariate analysis | | Multivariate analysis | | |
|---|---|---|---|---|---|
| | n = 77 | *P* value | HR | 95% CI | *P* value |
| GREB1 | | | | | |
| <30 | 40 | .03 | 13 | 1.61-312.4 | .01 |
| ≥30 | 37 | | | | |
| Age (y) | | | | | |
| <64 | 41 | .37 | 0.63 | 0.13-2.96 | .55 |
| ≥64 | 36 | | | | |
| Gender | | | | | |
| Male | 52 | .55 | 0.44 | 0.10-1.77 | .24 |
| Female | 25 | | | | |
| pT | | | | | |
| <3 | 7 | .94 | 1.99 | 0.13-110 | .65 |
| ≥3 | 70 | | | | |
| pN | | | | | |
| <1 | 39 | .08 | 2.38 | 0.53-10.9 | .24 |
| ≥1 | 38 | | | | |
| Tumor location | | | | | |
| Right sided | 11 | .6 | 0.62 | 0.02-4.71 | .69 |
| Left sided | 66 | | | | |
| Histologic type | | | | | |
| Well/moderate | 73 | .14 | 35.6 | 0.73-2713 | .06 |
| Poorly | 4 | | | | |
| Ly | | | | | |
| <Ly2 | 60 | .03 | 16.1 | 1.11-278 | .04 |
| ≥Ly2 | 12 | | | | |
| V | | | | | |
| <V2 | 60 | .99 | 1.06 | 0.06-12.8 | .96 |
| ≥V2 | 11 | | | | |

Abbreviations: CI, confidence interval; HR, hazard ratio; Ly, lymphatic invasion; V, venous invasion.

activation domains, the ligand-independent AF-1 domain, and the ligand-dependent AF-2 domain.[29,30] Estrogen receptor has been classically thought to be activated by the ligand-dependent pathway.

Recently, a ligand-independent pathway has also been reported. In response to the activation of the MAPK pathway, phosphorylation occurs on Ser118, which is located in the AF-1 domain of ER, and its phosphorylation provides an important mechanism that regulates AF-1 activity.[31,32] Moreover, activation of RAS-RAF-MAPK signaling by this ligand-independent pathway has been reported as a mechanism of TAM resistance in ER-positive breast cancer as well as HGSOC.[33,34] In ER-positive breast cancer, there was a correlation between TAM resistance and expression of phosphorylated RAF (ser338). In the case of ER-positive HGSOC, TAM resistance was correlated with phosphorylated MAPK expression, which was reversed by a MEK inhibitor (selumetinib).[33,34] Based on these findings, phosphorylating ER-Ser118 in AF-1 activated by the RAS-RAF-MAPK signal was detected as a TAM-resistant mechanism, suggesting that a ligand-independent ER pathway might play an important role in carcinogenesis as the downstream pathway of activated RAF.

As *GREB1* was upregulated by either $BRAF^{V600E}$ or $KRAS^{G12D}$ mutation in GEMMs and human CRC cell lines, it was expected that activation of the KRAS-BRAF-MAPK axis might induce estradiol-independent ER activation, resulting in oncogenic *GREB1* upregulation. Although we have tried to demonstrate ER phosphorylation by $BRAF^{V600E}$, the Abs for ER and phospho-ER are not capable of detecting endogenous proteins, as the *ER*-mRNA expression levels in CRC cell lines are 2000 times lower than in breast cancer cell lines by qRT-PCR (Figure S3).

In conclusion, we found that $BRAF^{V600E}$ mutation led to upregulation of GREB1 expression, which promoted tumor cell proliferation in colorectal tumorigenesis. Although the mechanism of GREB1 expression was reported to be controlled by estradiol-independent phosphorylation of ER through $BRAF^{V600E}$ mutation in some breast cancer cell lines, we could not determine a similar mechanism in human CRC cell lines. However, even though this question should be addressed by other methods, the *GREB1* knockdown in vivo transplantation model showed remarkable reduction of tumors and is thus a potential candidate molecular target for the treatment of $BRAF^{V600E}$-mutated CRCs.

## ACKNOWLEDGMENTS

This work was undertaken at the Analysis Center of Life Science and the Research Facilities for Laboratory Animal Science, Natural Science Center for Basic Research and Development (NBARD), Hiroshima University. Special thanks to Tsuneo Ikenoue MD, PhD and Hidehiko Takigawa MD, PhD for technical support, Yuko Ishida for technical assistance, and Minoru Hattori, PhD for statistical support. The results shown here are, in part, based on data generated by TCGA Research Networks (http://www.cancer.gov/tcga). This work was supported by JSPS KAKENHI Grant Numbers JP22390257 (2010-2012), JP25293284 (2013-2016), and JP18K08694 (2018-2021) and by The Japanese Society of Gastroenterology Grant-in-Aid 2010.

## CONFLICT OF INTEREST

The authors declare no potential conflicts of interest.

## ORCID

*Masatoshi Kochi* https://orcid.org/0000-0002-2113-1734
*Takao Hinoi* https://orcid.org/0000-0003-0462-6177
*Yasufumi Saito* https://orcid.org/0000-0002-0407-7684
*Kazuhiro Sentani* https://orcid.org/0000-0002-8987-5414
*Wataru Yasui* https://orcid.org/0000-0002-8647-8405

## REFERENCES

1. Fearon ER, Vogelstein B. A genetic model for colorectal tumorigenesis. *Cell*. 1990;61:759-767.
2. Vogelstein B, Papadopoulos N, Velculescu VE, Zhou S, Diaz LA Jr, Kinzler KW. Cancer genome landscapes. *Science*. 2013;339:1546-1558.
3. Bardelli A, Siena S. Molecular mechanisms of resistance to cetuximab and panitumumab in colorectal cancer. *J Clin Oncol*. 2010;28:1254-1261.
4. Heinemann V, von Weikersthal LF, Decker T, et al. FOLFIRI plus cetuximab versus FOLFIRI plus bevacizumab as first-line treatment for patients with metastatic colorectal cancer (FIRE-3): a randomised, open-label, phase 3 trial. *Lancet Oncol*. 2014;15:1065-1075.
5. Schwartzberg LS, Rivera F, Karthaus M, et al. PEAK: a randomized, multicenter phase II study of panitumumab plus modified fluorouracil, leucovorin, and oxaliplatin (mFOLFOX6) or bevacizumab plus mFOLFOX6 in patients with previously untreated, unresectable, wild-type KRAS exon 2 metastatic colorectal cancer. *J Clin Oncol*. 2014;32:2240-2247.
6. Bahrami A, Hesari A, Khazaei M, Hassanian SM, Ferns GA, Avan A. The therapeutic potential of targeting the BRAF mutation in patients with colorectal cancer. *J Cell Physiol*. 2018;233:2162-2169.
7. Davies H, Bignell GR, Cox C, et al. Mutations of the BRAF gene in human cancer. *Nature*. 2002;417:949-954.
8. Corcoran RB, Ebi H, Turke AB, et al. EGFR-mediated re-activation of MAPK signaling contributes to insensitivity of BRAF mutant colorectal cancers to RAF inhibition with vemurafenib. *Cancer Discov*. 2012;2:227-235.
9. Prahallad A, Sun C, Huang S, et al. Unresponsiveness of colon cancer to BRAF(V600E) inhibition through feedback activation of EGFR. *Nature*. 2012;483:100-103.
10. Kopetz S, Desai J, Chan E, et al. Phase II pilot study of vemurafenib in patients with metastatic BRAF-mutated colorectal cancer. *J Clin Oncol*. 2015;33:4032-4038.
11. Yaeger R, Cercek A, O'Reilly EM, et al. Pilot trial of combined BRAF and EGFR inhibition in BRAF-mutant metastatic colorectal cancer patients. *Clin Cancer Res*. 2015;21:1313-1320.
12. Hong DS, Morris VK, El Osta B, et al. Phase IB study of vemurafenib in combination with irinotecan and cetuximab in patients with metastatic colorectal cancer with BRAFV600E mutation. *Cancer Discov*. 2016;6:1352-1365.
13. Toyota M, Ahuja N, Ohe-Toyota M, Herman JG, Baylin SB, Issa JP. CpG island methylator phenotype in colorectal cancer. *Proc Natl Acad Sci USA*. 1999;96:8681-8686.
14. Ogino S, Nosho K, Kirkner GJ, et al. CpG island methylator phenotype, microsatellite instability, BRAF mutation and clinical outcome in colon cancer. *Gut*. 2009;58:90-96.
15. Akyol A, Hinoi T, Feng Y, Bommer GT, Glaser TM, Fearon ER. Generating somatic mosaicism with a Cre recombinase-microsatellite sequence transgene. *Nat Methods*. 2008;5:231-233.
16. Feng Y, Sentani K, Wiese A, et al. Sox9 induction, ectopic Paneth cells, and mitotic spindle axis defects in mouse colon adenomatous epithelium arising from conditional biallelic Apc inactivation. *Am J Pathol*. 2013;183:493-503.
17. Niitsu H, Hinoi T, Kawaguchi Y, et al. KRAS mutation leads to decreased expression of regulator of calcineurin 2, resulting in tumor proliferation in colorectal cancer. *Oncogenesis*. 2016;5:e253.
18. Kawaguchi Y, Hinoi T, Saito Y, et al. Mouse model of proximal colon-specific tumorigenesis driven by microsatellite instability-induced Cre-mediated inactivation of Apc and activation of Kras. *J Gastroenterol*. 2016;51:447-457.
19. Dankort D, Filenova E, Collado M, Serrano M, Jones K, McMahon M. A new mouse model to explore the initiation, progression, and therapy of BRAFV600E-induced lung tumors. *Genes Dev*. 2007;21:379-384.
20. Hinoi T, Lucas PC, Kuick R, Hanash S, Cho KR, Fearon ER. CDX2 regulates liver intestine-cadherin expression in normal and malignant colon epithelium and intestinal metaplasia. *Gastroenterology*. 2002;123:1565-1577.
21. Miguchi M, Hinoi T, Shimomura M, et al. Gasdermin C is upregulated by inactivation of transforming growth factor beta receptor type II in the presence of mutated Apc, promoting colorectal cancer proliferation. *PLoS One*. 2016;11:e0166422.
22. Hinoi T, Loda M, Fearon ER. Silencing of CDX2 expression in colon cancer via a dominant repression pathway. *J Biol Chem*. 2003;278:44608-44616.
23. Nagase T, Ishikawa K, Miyajima N, et al. Prediction of the coding sequences of unidentified human genes. IX. The complete sequences of 100 new cDNA clones from brain which can code for large proteins in vitro. *DNA Res*. 1998;5:31-39.
24. Rae JM, Johnson MD, Scheys JO, Cordero KE, Larios JM, Lippman ME. GREB 1 is a critical regulator of hormone dependent breast cancer growth. *Breast Cancer Res Treat*. 2005;92:141-149.
25. Fung JN, Holdsworth-Carson SJ, Sapkota Y, et al. Functional evaluation of genetic variants associated with endometriosis near GREB1. *Hum Reprod*. 2015;30:1263-1275.
26. Laviolette LA, Hodgkinson KM, Minhas N, Perez-Iratxeta C, Vanderhyden BC. 17beta-estradiol upregulates GREB1 and accelerates ovarian tumor progression in vivo. *Int J Cancer*. 2014;135:1072-1084.
27. Hnatyszyn HJ, Liu M, Hilger A, et al. Correlation of GREB1 mRNA with protein expression in breast cancer: validation of a novel GREB1 monoclonal antibody. *Breast Cancer Res Treat*. 2010;122:371-380.
28. Rae JM, Johnson MD, Cordero KE, et al. GREB1 is a novel androgen-regulated gene required for prostate cancer growth. *Prostate*. 2006;66:886-894.
29. Warnmark A, Treuter E, Wright AP, Gustafsson JA. Activation functions 1 and 2 of nuclear receptors: molecular strategies for transcriptional activation. *Mol Endocrinol*. 2003;17:1901-1909.
30. Sun J, Nawaz Z, Slingerland JM. Long-range activation of GREB1 by estrogen receptor via three distal consensus estrogen-responsive elements in breast cancer cells. *Mol Endocrinol*. 2007;21:2651-2662.
31. Yamashita H, Nishio M, Kobayashi S, et al. Phosphorylation of estrogen receptor alpha serine 167 is predictive of response to endocrine therapy and increases postrelapse survival in metastatic breast cancer. *Breast Cancer Res*. 2005;7:R753-764.
32. Murphy L, Cherlet T, Adeyinka A, Niu Y, Snell L, Watson P. Phosphoserine-118 estrogen receptor-alpha detection in human breast tumors in vivo. *Clin Cancer Res*. 2004;10:1354-1359.
33. Hew KE, Miller PC, El-Ashry D, et al. MAPK activation predicts poor outcome and the MEK inhibitor, selumetinib, reverses antiestrogen resistance in ER-positive high-grade serous ovarian cancer. *Clin Cancer Res*. 2016;22:935-947.
34. McGlynn LM, Tovey S, Bartlett JM, Doughty J, Cooke TG, Edwards J. Interactions between MAP kinase and oestrogen receptor in human breast cancer. *Eur J Cancer*. 2013;49:1176-1186.

## SUPPORTING INFORMATION

Additional supporting information may be found online in the Supporting Information section.

**How to cite this article:** Kochi M, Hinoi T, Niitsu H, et al. Oncogenic mutation in RAS-RAF axis leads to increased expression of *GREB1*, resulting in tumor proliferation in colorectal cancer. *Cancer Sci*. 2020;111:3540–3549. https://doi.org/10.1111/cas.14558